Optical properties of polymer blends composed of Poly(methyl methacrylate) and Ethylene-vinyl acetate copolymer

Shuji Takahashi,[1,2)] Hiroaki Okada,[1)] Shogo Nobukawa,[1)] and Masayuki Yamaguchi[1)]

1) School of Materials Science, Japan Advanced Institute of Science and Technology
1-1 Asahidai, Nomi, Ishikawa 923-1292 JAPAN

2) Development Department, Suzuki Motor Corporation
300 Takatsuka-cho, Minami-ku, Hamamatsu, Shizuoka 432-8611 JAPAN

*Corresponding to
Masayuki Yamaguchi
School of Materials Science, Japan Advanced Institute of Science and Technology
1-1 Asahidai, Nomi, Ishikawa 923-1292 Japan
Phone +81-761-51-1621, Fax +81-761-51-1625
E-mail m_yama@jaist.ac.jp

Abstract

Optical properties for immiscible polymer blends composed of poly(methyl methacrylate), PMMA, and ethylene-vinyl acetate copolymer, EVA, are studied employing various EVA samples with different vinyl acetate contents. PMMA/EVA shows transparency at room temperature when the difference in refractive index between both phases is small. The light transmittance, however, decreases with increasing the ambient temperature. This phenomenon is attributed to the difference in the volume expansion ratio, leading to the difference in refractive index, between PMMA and EVA. It is found that addition of tricresyl phosphate, TCP, improves the transparency and its temperature dependence. As a result, a ternary PMMA/EVA/TCP blend shows high level of transparency in the wide temperature range, although it has apparent phase separated morphology.

Key words: polymer blends; transparency; refractive index

Introduction

Transparent polymers have been widely used in various fields such as industrial, medical, and household applications. In particular, poly(methyl methacrylate) (PMMA) is one of the most available polymers, because it has remarkable light transmittance, good weatherability, low refractive index and small birefringence compared to other transparent polymers. However, the applications required for high impact strength have been limited because of its inherent brittleness. In the 1970's, rubber toughening technology was proposed to improve the disadvantage.[1-4]

In case of rubber-toughened plastics using a transparent polymer, however, it is significantly difficult to keep the transparency because of the light scattering at the interface between two materials due to the difference in the refractive index.[5,6] Furthermore, it has been known that the light scattering can be reduced by adjusting the refractive indices of both phases.[7-9] Ethylene-vinyl acetate copolymer (EVA), known as a rubbery material because of the low degree of crystallization, is a good candidate for the modifier of PMMA, because the refractive index of EVA is very close to that of PMMA. Furthermore, the refractive index of EVA can be controlled by the vinyl acetate content.[10,11]

Up to now, several studies have been carried out on PMMA/EVA blends such as in-situ polymerization[12-14] and melt-mixing[15,16] in order to improve the impact property without losing transparency. Cheng et al. found that EVA-*g*-PMMA prepared by in-situ polymerization results in the fine dispersed EVA particles in the PMMA matrix.[13] Poomalai et al. reported that binary blends of PMMA/EVA in different proportions prepared by a melt-mixing method show a substantial increase in its impact strength from 19 to 32 J/m.[16] Bernini et al. evaluated the transparency as a function of

temperature using PMMA/EVA blends and found that PMMA/EVA shows a transparent-to-opaque transition at about 50 ^{o}C.[17,18] Moreover, Errico et al. revealed that the blend composed of EVA-*g*-PMMA and PMMA shows transparency at room temperature, while it becomes opaque at high temperature. They concluded that this phenomenon is attributed to the difference in the temperature dependence of refractive index between the graft copolymer and PMMA.[19] In general, the temperature coefficient of the refractive index (dn/dT) of a rubber is larger than that of a glassy polymer, because of a large value of the thermal expansion coefficient.[20] Therefore, the difference in the refractive index is dependent on the temperature. Furthermore, the crystallinity of EVA also plays an important role in the transparency because it affects the refractive index. It has been already clarified that the degree of crystallinity of EVA decreases with increasing the vinyl acetate content and becomes zero at approximately 25 wt%.[11]

The temperature dependence of the refractive index is expressed by the Lorentz and Lorenz equation.[21]

$$\frac{\partial n}{\partial T} = (n-1)\left[\frac{1}{\rho}\frac{\partial \rho}{\partial T} + \frac{1}{[R]}\frac{\partial [R]}{\partial T}\right] \tag{1}$$

$$\frac{1}{\rho}\frac{\partial \rho}{\partial T} = -3\alpha \tag{2}$$

where n the refractive index, T the temperature, ρ the density, [R] the molecular refractive and α the linear expansion coefficient. The equation shows that the temperature coefficient of the refractive index depends on the molecular refractive determined by the chemical structure and the molar volume.

In this study, a modification method of transparency by adding a liquid compound, tricresyl phosphate (TCP), to a binary blend composed of PMMA and EVA is demonstrated. TCP is a low-molecular compound with high refractive index and shows a plasticizing performance for PMMA and EVA. That is to say, to achieve high level of transparency in the wide temperature range, TCP should be added to the binary blend. Furthermore, the temperature dependence of transparency is investigated for the binary blends to clarify the relation between transparency and the difference in the refractive index.

Experimental

Materials

Polymers used in this study were commercially available poly(methyl methacrylate) (PMMA) (Sumitomo Chemical, Sumipex LG-21) and four types of ethylene-vinyl acetate copolymer (EVA) containing from 14 to 32 weight percent of vinyl acetate (VAc). The number-average molecular weight and polydispersity of PMMA are as follows; Mn = 4.4 x 10^4 and Mw/Mn = 1.89. The characteristics of EVA samples were summarized in Table 1. In this study, EVA14 represents EVA containing 14 wt% of vinyl acetate. Tricresyl phosphate (TCP, Daihachi Chemical Industry) was also employed. The refractive index at room temperature is 1.557.

[Table 1]

Sample Preparation

PMMA and EVA were mechanically blended with and without TCP in the molten state with thermal stabilizers such as hindered phenol (Ciba, Irganox 1010) and phosphate (Ciba, Irgafos 168). The blend ratio of the binary blends was PMMA/EVA = 80/20 in a weight fraction. In case of the ternary blends, the ratio was PMMA/EVA/TCP = 72/18/10 in a weight fraction. The amount of each thermal stabilizer used in the preparation was 0.5 %. Compounding was performed by an internal batch mixer (Toyoseiki, Labo-plastmil) at 200 ºC for 10 min. The blade rotation speed was 40 rpm. Prior to melt-mixing, the polymers were dried under vacuum at 60 ºC for 3 h. Furthermore, PMMA/TCP and EVA/TCP with various blend ratios were prepared by the same method.

The obtained samples were compressed into flat sheets with 0.2 mm thickness by a laboratory compression-molding machine at 200 ºC under 10 MPa for 10 min. Then the sample was subsequently cooled at 20 ºC for 5 min.

Measurements

Thermal analysis of EVA was conducted by a differential scanning calorimeter (DSC) (Mettler, DSC820) under a nitrogen atmosphere. The samples were heated from -80 to 120 ºC at a heating rate of 10 ºC/min to detect the melting point. After holding at 120 ºC for 3 min, the samples were cooled down to -80 ºC at a cooling rate of 10 ºC/min to detect the crystallization temperature. The amount of the sample in an aluminum pan was approximately 10 mg.

Refractive index was measured at 20 ºC and 70 ºC by an Abbe refract meter (ATAGO, NAR-1T) with methylene iodide as a contact liquid. Besides the EVA samples in Table 1, low-density polyethylene (LDPE) (Mitsui Chemical, 16P) and

poly(vinyl acetate) (PVAc) (Aldrich) were employed as polymers with 0 and 100 wt% of VAc content, respectively.

The temperature dependence of oscillatory tensile modulus in the solid state, such as tensile storage modulus E' and loss modulus E'', was measured by a dynamic mechanical analyzer (UBM, E4000) in the temperature range between -80 and 150 ºC. The heating rate was 2 ºC/min, and the applied frequency was 10 Hz. The rectangular samples with the dimension of 4 x 25 x 0.2 mm were cut out from the compressed flat sheets.

To evaluate the transparency and its temperature dependence of polymer blends, light transmittance was measured at various temperatures using an optical microscope (Leica microsystems, DMLP) equipped with a hot stage (Mettler, FP900) and a photo multiplier as a light detector. The light transmittance T is determined by the following relation:

$$T\ (\%) \ = \ I \ / \ I_0 \times 100 \qquad (3)$$

where I_0 and I are the intensities of transmittance light and incident light, respectively.

The morphology of the blends was examined by a scanning electron microscope (SEM) (Hitachi, S4100). Prior to the observation, the surface of cryogenically fractured samples was coated by Pt-Pd.

The linear thermal expansion coefficient was measured by a thermo-mechanical analyzer (TMA) (Brucker, TMA4000SA) in the temperature range between 20 and 80 ºC. The heating rate was 2 ºC/min. The rectangular samples with the dimension of 5 x 5 x 0.2 mm were cut out from the compressed flat sheets.

Results and Discussion

Characteristics of pure polymers

Table 2 shows the glass transition temperature (Tg), crystallization temperature (Tc), and melting point (Tm) of the EVA samples, which are determined by the DSC measurement. As seen in the table, all EVA samples show the same Tg, suggesting that they have the alomost same VAc content in the amorphous region. Furthermore, it is found from Figure 1 that Tc and Tm decrease with increasing the VAc content because of the decrease in the ethylene sequence, as firstly reported by Slayer et al.[10] On the other hand, Tg of PMMA is 105 ºC.

[Table 2] & [Figure 1]

Figure 2 shows the refractive index of EVA as a function of VAc content at 20 ºC. In the figure, the refractive index of LDPE, 1.5150, is also shown as an EVA sample containing 0 wt% of VAc. Moreover, the refractive index of PMMA, 1.4900, is shown by a solid line.

[Figure 2]

As seen in Figure 2, the refractive index decreases with VAc content because of low degree of crystallinity, and approaches to the value of PVAc, 1.4699. Furthermore, the refractive index of EVA25 is almost the same as that of PMMA. Therefore, it can be

deduced that the binary blend composed of PMMA and EVA25 is fairly transparent irrespective of the morphology.

Morphology and dynamic mechanical properties of binary blends

Figure 3 shows the SEM pictures of the cryogenically fractured surface of PMMA/EVA binary blends.

[Figure 3]

As seen in the figure, phase separated morphology is detected in all blends, in which spherical droplets of EVA are dispersed in a continuous phase of PMMA. The diameter of dispersed particles is in the range of 1-10 μm and almost the same irrespective of the VAc content.

Figure 4 exemplifies the temperature dependence of oscillatory tensile moduli such as storage modulus E' and loss moduli E'' in the solid state at 10 Hz for PMMA/EVA14.

[Figure 4]

The storage modulus E' decreases slightly around -40 ºC because of the glass-to-rubber transition of EVA phase. Then, E' drops off sharply around at 100 ºC due to Tg of PMMA phase. Correspondingly, there are two peaks in the loss modulus E'' curve, demonstrating that the blend shows phase separation. Furthermore, the locations of the peak temperature of E'' for the blend are the same as those for the individual pure components, which is confirmed also for the other binary blends. These

results demonstrate that molecules of EVA employed in this study are not dissolved into PMMA, even though PVAc is miscible with PMMA.[22]

Optical properties of binary blends

Figure 5 shows the light transmittance for the binary blends of PMMA and EVA at various temperatures. The content of EVA is 20 wt%.

[Figure 5]

The blend with EVA25 is the most transparent at 20 ºC. This is reasonable because EVA25 (n = 1.4902) shows the closest refractive index with PMMA (n = 1.4900). Nevertheless, it is demonstrated that the transmittance decreases with the ambient temperature. On the contrary, the transparency is improved at high temperature for PMMA/EVA14, although the blend is opaque at 20 ºC. This phenomenon is attributed to the difference in the thermal expansion coefficient and thus the temperature dependence of refractive index between PMMA and EVA, which is provided by the Lorentz and Lorenz equation. As shown in eq. (1), $\partial n/\partial T$ is determined by two terms, i.e., thermal expansion and molecular refractive, although the molecular refractive is hardly affected by temperature.[23] The thermal expansion of a rubbery material is generally larger than that of a glassy polymer. In fact, the temperature coefficients of the refractive index at λ = 514 nm and T = 20 ºC are -1.2 x 10^{-4} ºC $^{-1}$ for PMMA and -5.0 x 10^{-4} ºC $^{-1}$ for EVA.[24] Consequently, the refractive index of EVA decreases rapidly with increasing temperature as compared to that of PMMA.

The refractive index is also measured at 70 ºC. It is found that the value of EVA14 (n = 1.4857) is almost identical to that of PMMA (n = 1.4853), even though EVA14 (n = 1.5001) shows a much higher value than PMMA (n = 1.4900) at 20 ºC. As a result, the light transmittance increases with temperature for PMMA/EVA14.

Optical properties of ternary blend

Although the light transmittance of PMMA/EVA14 is the lowest among the binary blends at 20 ºC, it is significantly improved by the addition of TCP, as demonstrated in Figure 6. Considering that the refractive index of TCP is 1.5570, which is higher than those of PMMA and EVA14, this can be explained by the change in the difference in the refractive index of both phases.

[Figure 6]

It should be noted in Figure 6 that the ternary blend with TCP shows high level of light transmittance in the broad range of temperature, even though the difference in the refractive index shows the largest among the binary blends at 20 ºC as shown in Figure 2. Upon the addition of TCP, the ternary blend shows approximately 90 % of the light transmittance at 20 ºC, which is almost the same value as PMMA/EVA25. Furthermore, it shows over 80 % even at 90 ºC. Consequently, the light transmittance of PMMA/EVA14/TCP exceeds 80 % in a wide temperature range from 20 ºC to 90 ºC.

In order to clarify the effect of TCP, refractive index of PMMA/TCP and EVA14/TCP at 20 ºC and 70 ºC are evaluated as shown in Figure 7. During the measurements, as similar to the ternary blends, the segregation of TCP on the surface of

the sample plates, which is called “bleeding-out” in industry, is not detected irrespective of the ambient temperature and the TCP content, at least, in this study.

[Figure 7]

It is found that refractive index of the blends linearly increases with TCP content because of the high refractive index of TCP. However, the slopes are strongly dependent upon the species of polymers and the temperature. The figure contains important information. Firstly, the difference in the refractive index at 20 ºC between PMMA/TCP and EVA14/TCP becomes small as TCP content increases, because the slope of PMMA/TCP (10.5×10^{-2} (calculated as a linear slope)) is larger than that of EVA14/TCP (4.2×10^{-2}). Secondly, the difference in the refractive index at 70 ºC between PMMA/TCP and EVA14/TCP keeps a small constant value, irrespective of TCP content, because the slope of PMMA/TCP (3.9×10^{-2}) is almost similar to that of EVA14/TCP (4.9×10^{-2}). These phenomena are responsible for the small difference in the refractive index between both phases in a wide temperature range.

Although the exact reason is not clarified, the molecular packing condition could be the possible mechanisms to explain the temperature dependence of refractive index, i.e., thermal expansion behaviors. In case of PMMA, rapid cooling from the molten state leads to loosed packing of molecules in the glassy state, i.e., low specific volume. Because of a large amount of free volume, the thermal expansion would be pronounced. As increasing TCP, however, temperature gap between Tg and the mold temperature of the compression-molding machine at the cooling process (20 ºC) becomes small due to the decrease in Tg. As a result, the specific volume and thus the free volume fraction of

PMMA tend to increase with increasing TCP content. Even if the temperature gap is not so important, the addition of a plasticizer tends to loosen the molecular packing. Up to now, the effect of the addition of a plasticizer on the thermal expansion has been reported by two research gropus to the best of our knowledge. Mohanty et al. found that the plasticized cellulose acetate shows enhanced thermal expansion.[25] Furthermore, Borek et al. revealed that free volume fraction of poly(vinyl chloride) (PVC) in the glassy state increases with a plasticizer.[26]

On the contrary, addition of TCP has no/little effect on the specific volume of EVA, because Tg of the amorphous region, in which TCP molecules must exist,[27] is significantly lower than 20 ºC even without TCP.

In general, anharmonicity of potential-energy function, which can be detected by vibrational frequency shift in the infrared and Raman spectra by applied stress,[28,29] is responsible for the thermal expansion. The thermal expansion, i.e., separation between the molecules with increasing temperature, occurs owing to the asymmetry of the potential function. When a material has strong anharmonicity with low modulus, it shows marked thermal expansion.[28-32] Since the modulus becomes lower by the additoon of TCP, pronounced thermal expansion is expected.

In order to examine the thermal expansion behavior directly, the linear expansion coefficient of PMMA and PMMA/TCP (90/10) is measured from 20 ºC to 80 ºC as shown in Figure 8. Furthermore, the refractive index of PMMA and PMMA/TCP (90/10) are calculated by eq. (1) using the data in Figure 8.

[Figure 8] & [Figure 9]

It is obvious that the linear expansion coefficient increases by the addition of TCP. Furthermore, the calculated value of the refractive index, as shown in Figure 9, at 70 ºC is 1.494, which approximately corresponds to the result (1.492) in Figure 7, the experimental data obtained by an Abbe refract meter.

Morphology and dynamic mechanical properties of blends with TCP

Figure 10 shows the peak temperature of E'' curves ascribed to the glass-to-rubber transition of PMMA/TCP and EVA14/TCP.

[Figure 10]

As seen in the figure, Tg's of PMMA and EVA14 decrease with TCP content monotonically in the experimental region. The slope of PMMA is slightly larger than that of EVA14, e.g., from 110 ºC (0 wt%) to 74 ºC (15 wt%) for PMMA and from -28 ºC (0 wt%) to -50 ºC (15 wt%) for EVA14.

Prior to the dynamic mechanical measurement of the PMMA/EVA14/TCP ternary blend, the blend morphology was checked by SEM using the cryogenically fractured surface as shown in Figure 11.

[Figure 11]

Apparently, phase separated morphology is detected in the blend, in which spherical droplets of EVA phase are dispersed in a continuous phase of PMMA, even though TCP is dissolved in both PMMA and EVA phases. Furthermore, the diameter of

dispersed particles is almost the same as that of the binary PMMA/EVA14 blend (Figure 3 (a)), irrespective of the addition of TCP.

Figure 12 shows the temperature dependence of the oscillatory tensile moduli for PMMA/EVA14/TCP.

[Figure 12]

As seen in the figure, E' decreases moderately in the low temperature region and falls off sharply around at 75 ºC. As compared with the binary blend without TCP, of course, the modulus drop starts at lower temperature. Both peaks of E'', i.e., Tg's of individual phases, are shifted to lower temperatures than those for the blend without TCP. The lower peak temperature, Tg of EVA phase, is observed at -32 ºC, which is almost identical to that of EVA14 with 5 wt% of TCP, as shown in Figure 10. This result suggests that the EVA phase in the ternary blend contains approximately 5 wt% of TCP below Tg of EVA. Thus, the PMMA phase contains 11.2 wt% of TCP. Therefore, the refractive indices of individual phases with TCP are calculated to be $n_{PMMA/TCP}$ = 1.502 and $n_{EVA14/TCP}$ = 1.503, respectively. Consequently, the ternary blend provides a high level of light transmittance below Tg of EVA, because the difference in the refractive index of each phase becomes small. On the other hand, the higher peak temperature, Tg of PMMA phase, is observed at 84 ºC. This is almost similar to that of PMMA with 10.8 wt% of TCP. Although there is a possibility of TCP transfer from PMMA to EVA14, as suggested by Min et al.[35] using PMMA/PVC/plasticizer blends, the present result indicates that TCP content in PMMA

phase is not so changed. As a result, the difference in refractive index at 70 ºC is also small (Figure 7), leading to good transparency.

Conclusions

The transparency and its temperature dependence for immiscible polymer blends composed of PMMA and EVA are studied. It is found that the difference in refractive index of each phase is the most important factor for transparency of the binary blends. However, the transparency of the binary blend depends on the ambient temperature to a great extent, because the temperature dependence of refractive index of EVA is more pronounced than that of PMMA.

Addition of TCP into the PMMA/EVA blend improves the transparency and its temperature dependence. This phenomenon can be explained by the following reasons; (1) The difference in the refractive index between both phases is reduced because of the high refractive index of TCP and (2) Addition of TCP increases the thermal expansion coefficient of PMMA.

In this paper, a new material design of transparent rubber-toughened polymer blends having phase separated morphology is demonstrated. However, the thermal and mechanical properties such as heat deflection temperature, toughness, and yield stress should be checked in detail prior to application, because the addition of plasticizers always provides a negative influence on these properties. A new plasticizer having large refractive index and appropriate solubility parameter should be preferred for industrial application, because a small amount is enough to control the refractive index.

References

(1) Ayre DS, Bucknall CB. Polymer 1998;39:4785-91.

(2) Gloaguen JM, Steer P, Gaillard P, Wrotecki C, Lefebvre JM. Polym Eng Sci 1993;33:748-53.

(3) Smith AP, Ade H, Balik CM, Koch CC, Smith SD, Spontak RG. Macromolecules 2000;33:2595-604.

(4) Poomalai P, Varghese TO, Siddramaiah J. J Appl Polym Sci 2008;109:3511-8.

(5) Huges LT, Britt GE. J Appl Polym Sci 1961;5:337-48.

(6) Roxton TR. J Appl Polym Sci 1963;7:1499-508.

(7) Song JY, Kim JW, Suh KD. J Appl Polym Sci 1999;71:1607-14.

(8) Park JY, Kim JY, Suh KD. J Appl Polym Sci 1998;69:2291-302.

(9) Feng J, Winnik MA, Shivers RR, Clubb B. Macromolecules 1995;28:7671-82.

(10) Salyer IO, Kenyon AS. J Polym Sci Part A 1971;9:3083-103.

(11) Arsac A, Carrot C, Guillet J. J Appl Polym Sci 1999;74:2625-30.

(12) Laurienzo P, Malinconico M, Matruscelli E, Ragosta G, Volpe MG. J Appl Polym Sci 1992;44:1883-92.

(13) Cheng SK, Chen CY. J Appl Polym Sci 2003;90:1001-8.

(14) Cheng SK, Chen CY. Eur Polym J 2004;40:1239-48.

(15) Poomalai P, Ramaraj B, Siddramaiah. J Appl Polym Sci 2007;104:3145-50.

(16) Poomalai P, Ramaraj B, Siddramaiah. J Appl Polym Sci 2007;106:684-91.

(17) Bernini U, Carbonara G, Malinconico M, Mormile P, Russo P, Volpe MG. Appl Opt 1992;31:5794-98.

(18) Bernini U, Malinconico M, Matruscelli E, Mormile P, Novellino A, Russo P, Volpe MG. J Mater Process Technol 1995;55:224-8.

(19) Errico ME, Greco R, Laurienzo P, Malinconico M, Viscardo D. J Appl Polym Sci 2006;99:2926-35.

(20) Zoller P, Walsh DJ. Technomic Lancaster PA 1995;147:91.

(21) Choi JH, Eichele C, Lin YC, Shi FG, Carlson R, Sciamanna S. Scripta Materialia 2008;58:413-6.

(22) Song M, Long F. Eur Polym J 1991;27:983-6.

(23) Bernini U, Stefano LD, Feo M, Mormile P, Russo P. Appl Phys B 1996;63:155-9.

(24) Bernini U, Malinconico M, Matruscelli E, Mormile P, Russo P, Volpe MG. J Mater Sci 1993;28:6399-402.

(25) Mohanty AK, Wibowo A, Misra M, Drzal LT. Polym Eng Sci 2003;43:1151-61.

(26) Borek J, Osoba W. J Polym Sci Polym Phys 1998;36:1839-45.

(27) Qian JW, An QF, Zhou GH. Eur Polym J 2003;39:375-9.

(28) Nitta K, Yamaguchi M. J Mater Sci 1998;33:1015-21.

(29) Yamaguchi M, Nitta K, Tanaka A, Kitamura M. J Polym Sci Polym Phys 1999;37:1513-21.

(30) Yamamoto O. Polym J 1971;2:501-17.

(31) Kijima T, Koga K, Imada K, Takayanagi M. Polym J 1975;7:14-20.

(32) Barron RM, Barron THK, Mummery PM, Sharkey M. Can J Chem 1988;66:718-24.

(33) Jarzynski J, Balizer E, Fedderyl J, Lee G. Acoustic Properties, in Properties and Behavior of Polymers, Vol.1, Seidel A. Ed., Wiley, New York, 2011.

(34) Hartwig G. Cryogenic Properties, in Properties and Behavior of Polymers, Vol.1, Seidel A. Ed., Wiley, New York, 2011.

(35) Min KE, Lim JC, Seo WY, Kwon HK. J Appl Polym Sci 1994;51:1521-25.

Figure Captions

Figure 1 Melting point Tm and crystallization temperature Tc plotted against VAc content in EVA; (circles) Tm and (diamonds) Tc.

Figure 2 Refractive index of EVA as a function of VAc content. The bold line represents the refractive index of PMMA.

Figure 3 Scanning electron micrographs of PMMA/EVA (80/20) blends; (a) PMMA/EVA14, (b) PMMA/EVA20, (c) PMMA/EVA25 and (d) PMMA/EVA32.

Figure 4 Temperature dependence of (opened circles) tensile storage modulus E' and (closed circles) loss modulus E'' at 10 Hz for PMMA/EVA14. In the figure, E'' curves around Tg of (triangles) EVA14 and (diamonds) PMMA are also shown with vertical shift.

Figure 5 Temperature dependence of light transmittance for binary blends containing 20 wt% of EVA; (circles) PMMA/EVA14, (squares) PMMA/EVA20, (diamonds) PMMA/EVA25 and (triangles) PMMA/EVA32.

Figure 6 Temperature dependence of light transmittance for (circles) PMMA/EVA14/TCP and (diamonds) PMMA/EVA14.

Figure 7 Refractive index plotted against the TCP content; (circles) PMMA/TCP and (diamonds) EVA14/TCP at (open symbols) 20 ºC and (closed symbols) 70 ºC.

Figure 8 Linear expansion coefficients of (closed circles) PMMA and (opened circles) PMMA/TCP (90/10).

Figure 9 Predicted linear expansion coefficients using the Lorentz and Lorentz equation for (closed circles) PMMA and (open circles) PMMA/TCP (90/10).

Figure 10 Relation between Tg and TCP content; (circles) PMMA/TCP and (diamonds) EVA14/TCP.

Figure 11 Scanning electron micrograph of PMMA/EVA14/TCP.

Figure 12 Temperature dependence of (opened circles) tensile storage modulus E' and (closed circles) loss modulus E'' at 10 Hz for PMMA/EVA14/TCP. In the figure, E'' curves around Tg of (triangles) EVA14/TCP (95/5) and (diamonds) PMMA/TCP (90/10) are also shown with vertical shift.

Table 1. Characteristics of EVA samples

Sample Code	VAc content (wt%)	MFR (g/10min)*
EVA14	14	15
EVA20	20	20
EVA25	25	2
EVA32	32	30

* 190ºC under 2.16kgf.

Table 2. Thermal properties of EVA samples

Sample Code	Tg (ºC)*	Tc (ºC)#	Tm (ºC) #
EVA14	-26	70	90
EVA20	-26	65	82
EVA25	-26	58	78
EVA32	-26	41	57

* Reference value of supplier (determined from DSC measurement)

Determined from DSC measurement.

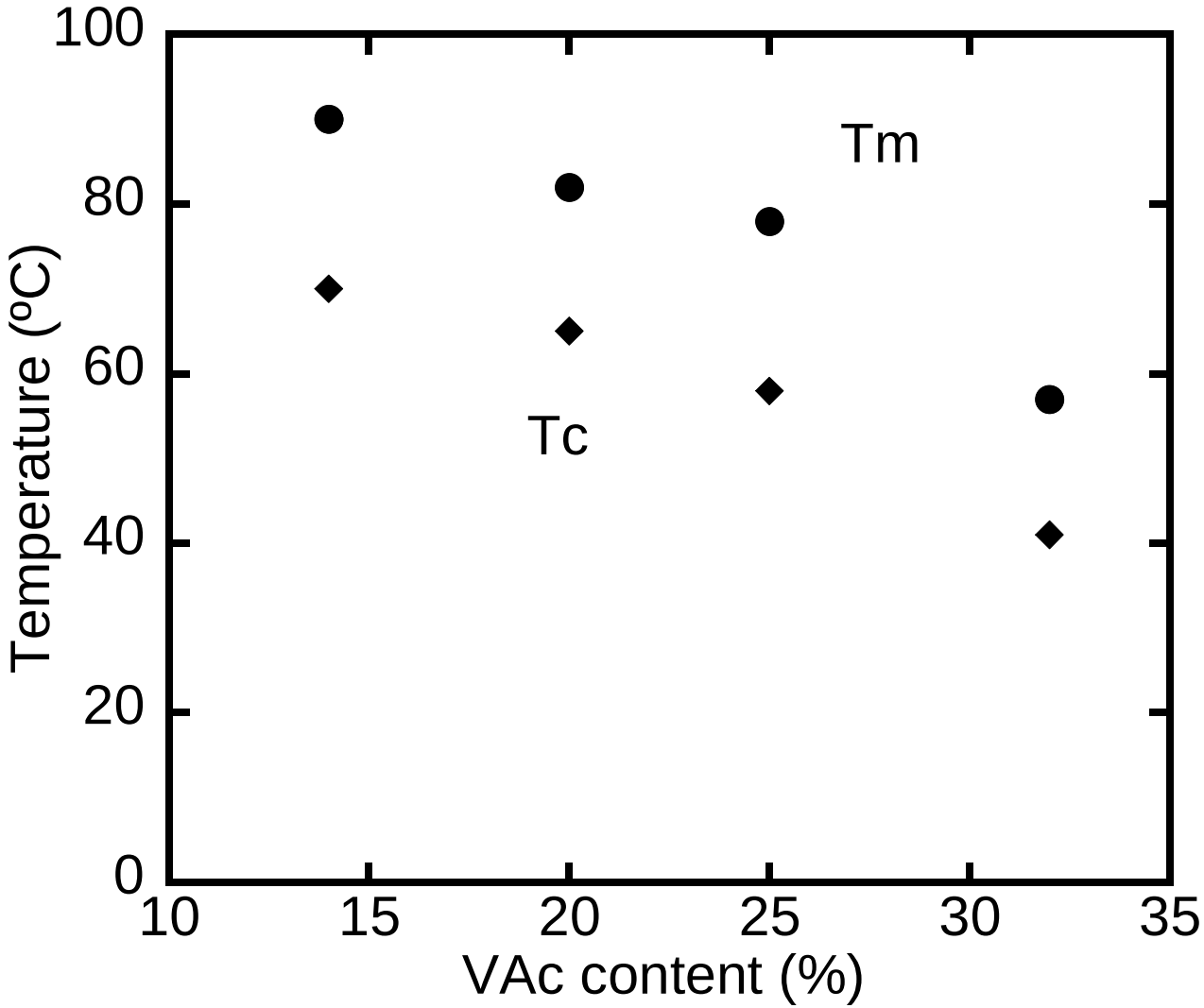

Takahashi et al.,

Figure 1

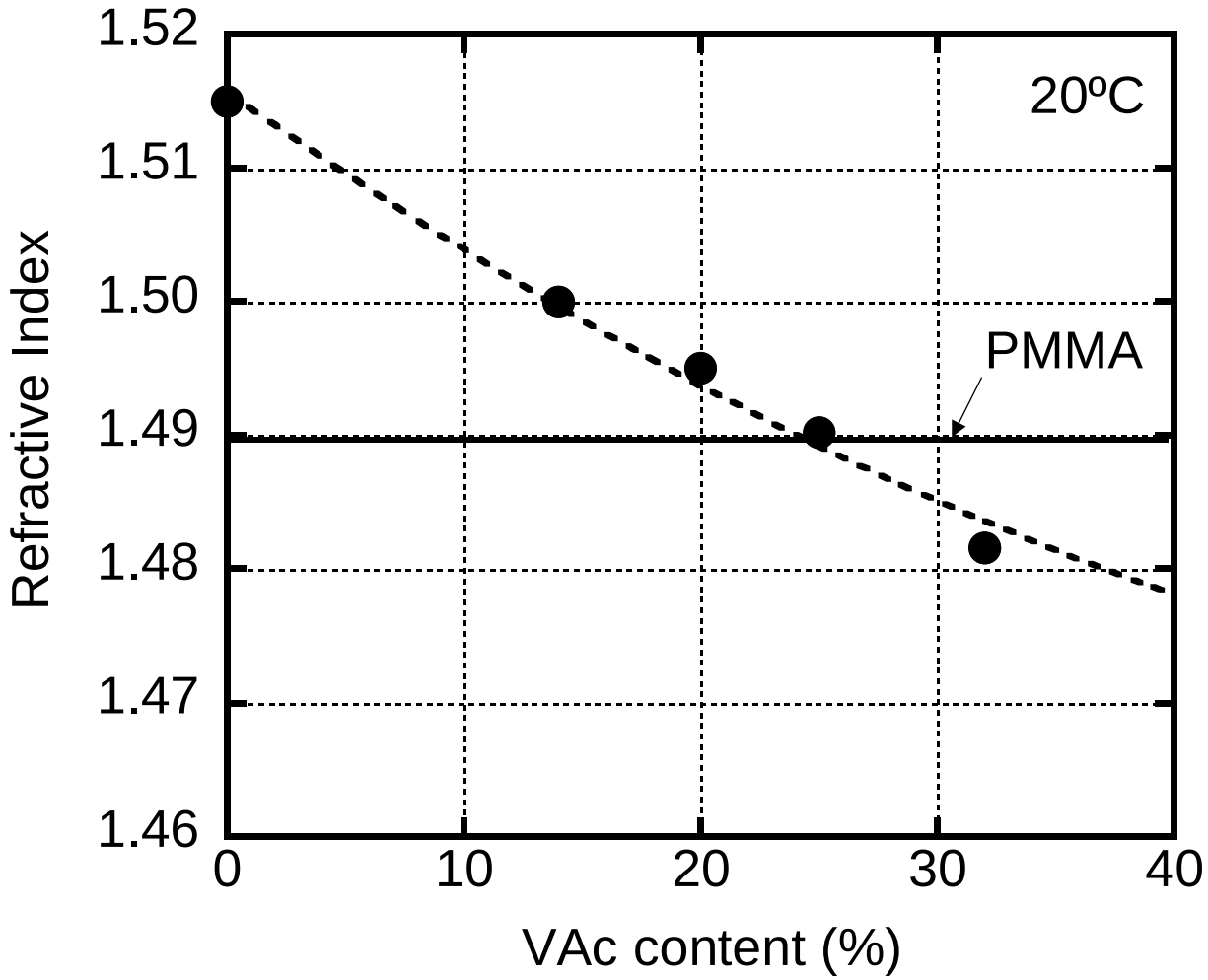

Takahashi et al.,

Figure 2

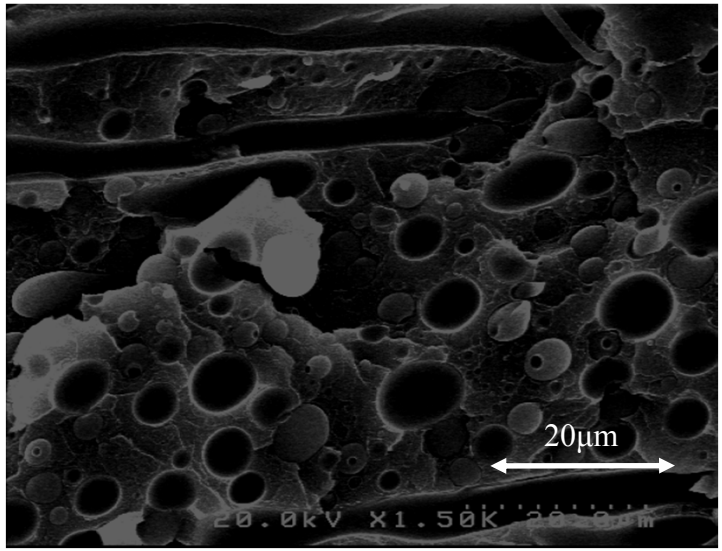

(a) PMMA/EVA14

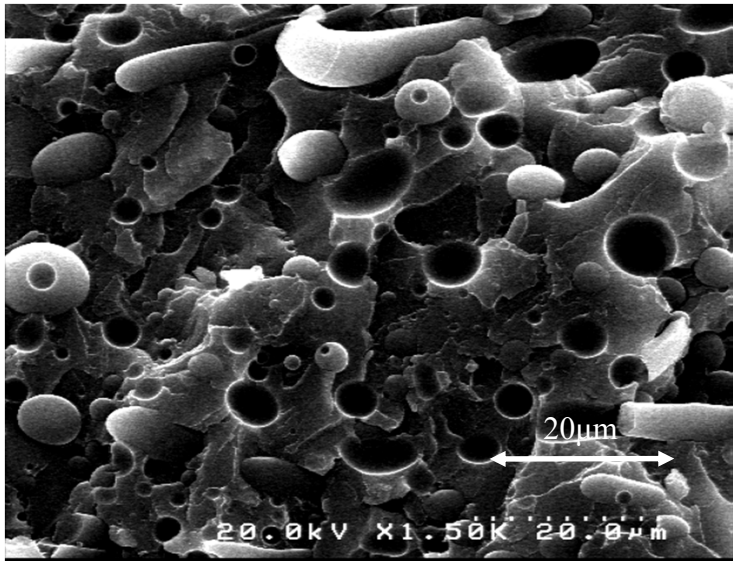

(b) PMMA/EVA20

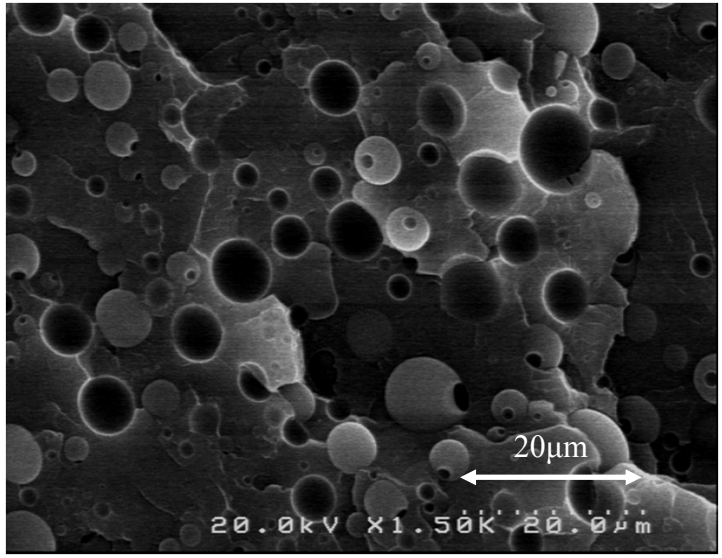

(c) PMMA/EVA25

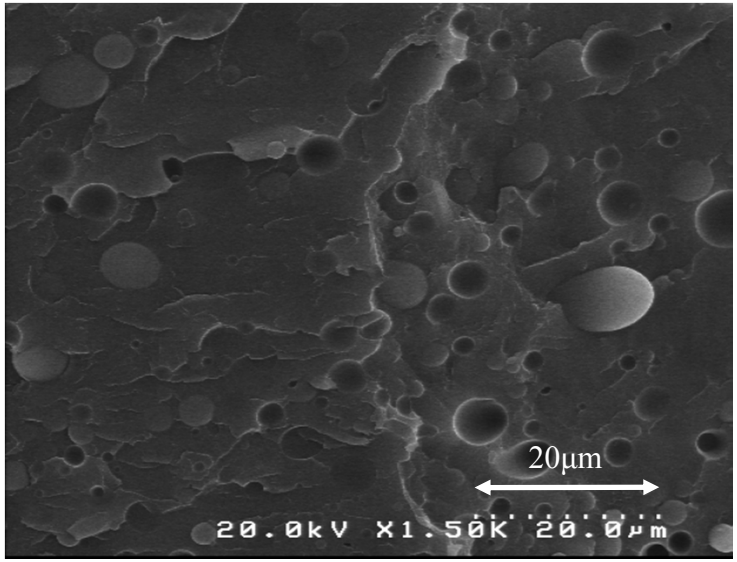

(d) PMMA/EVA32

Takahashi et al.,

Figure 3

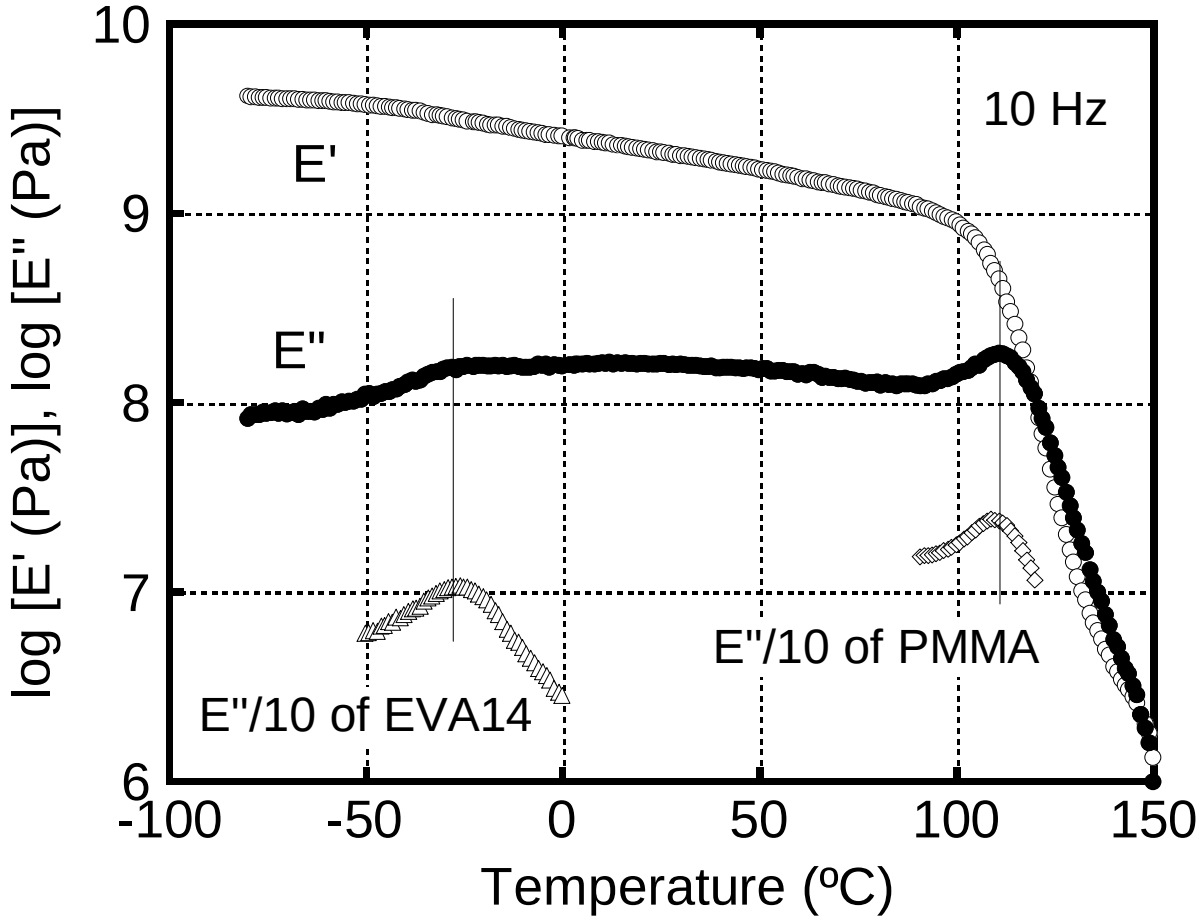

Takahashi et al.,

Figure 4

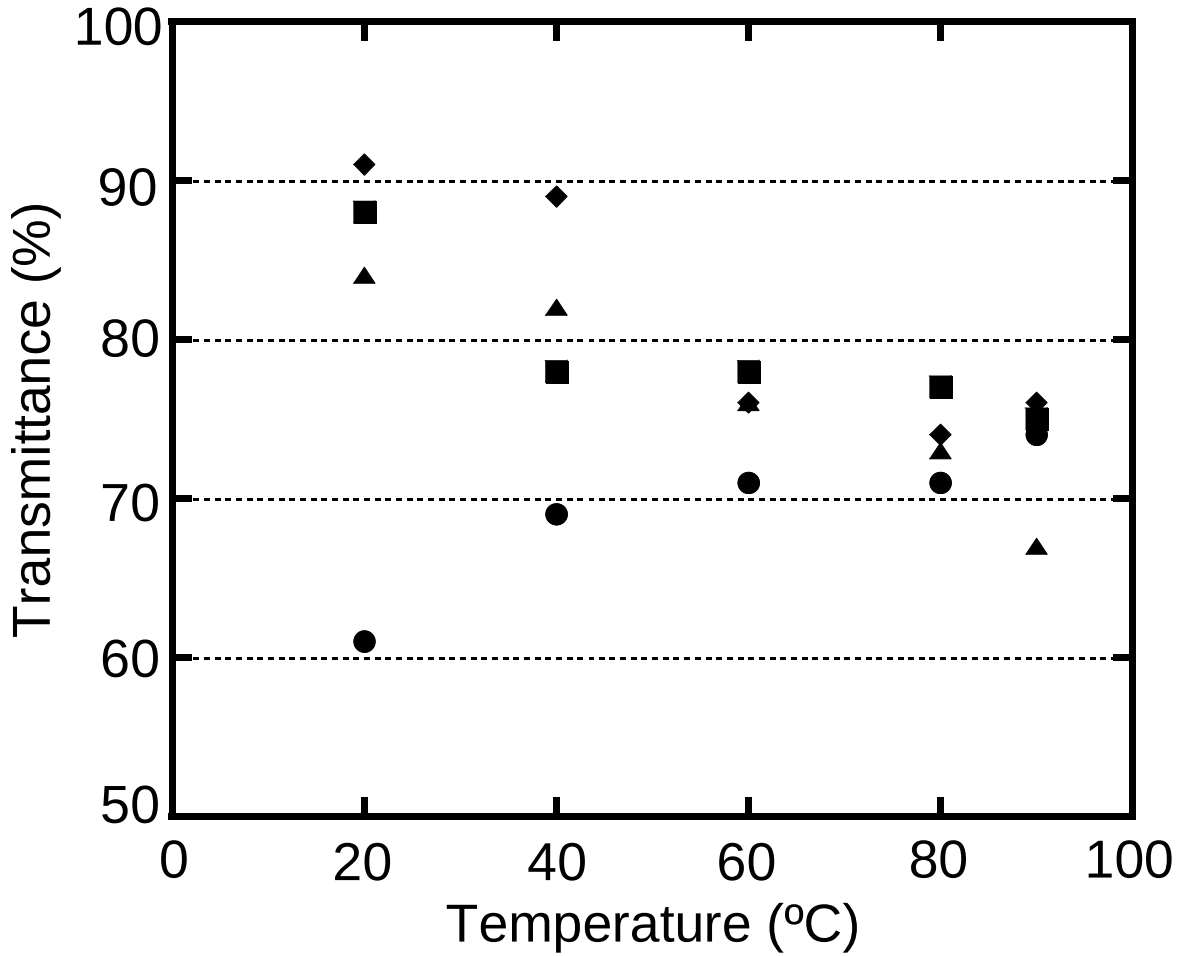

Takahashi et al.,

Figure 5

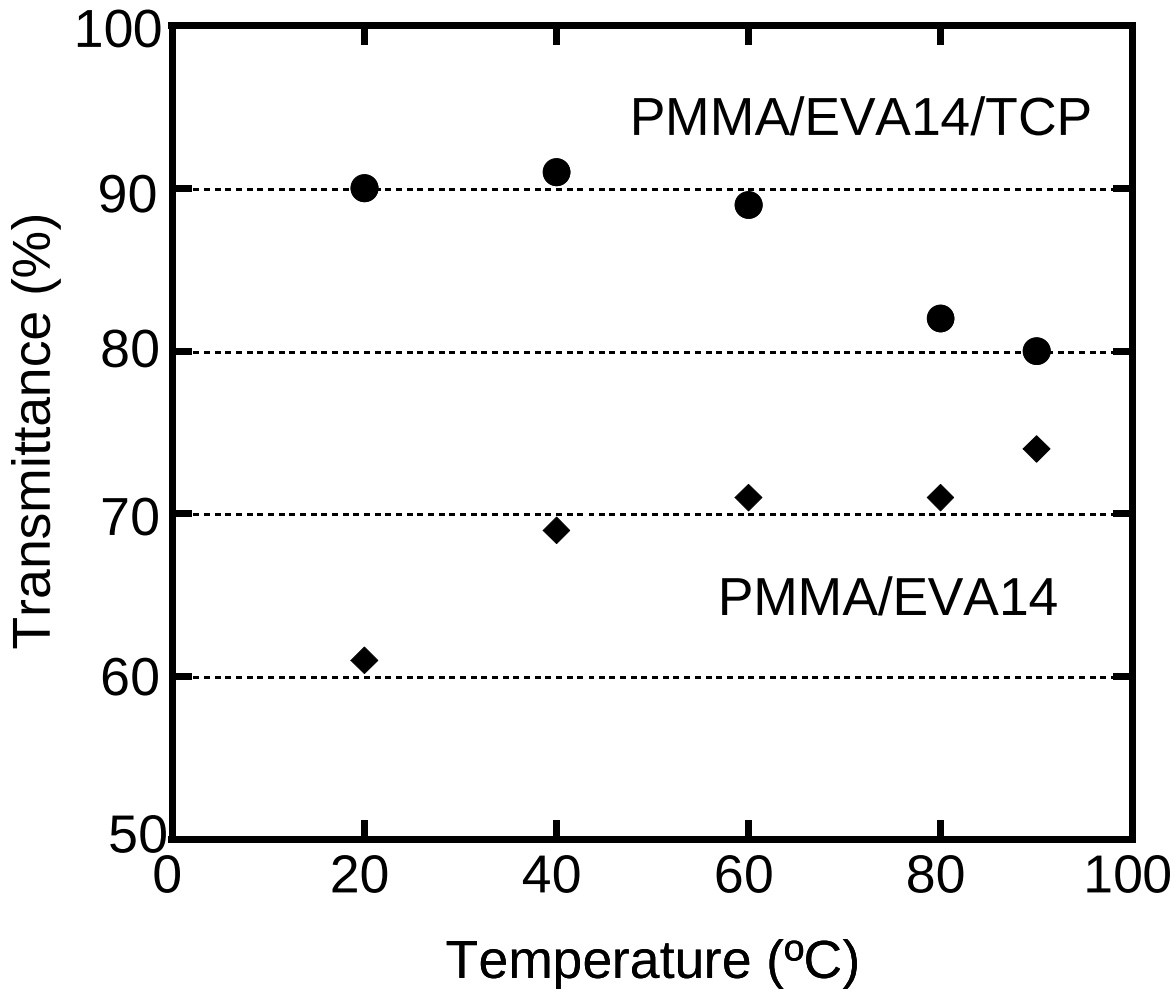

Takahashi et al.,

Figure 6

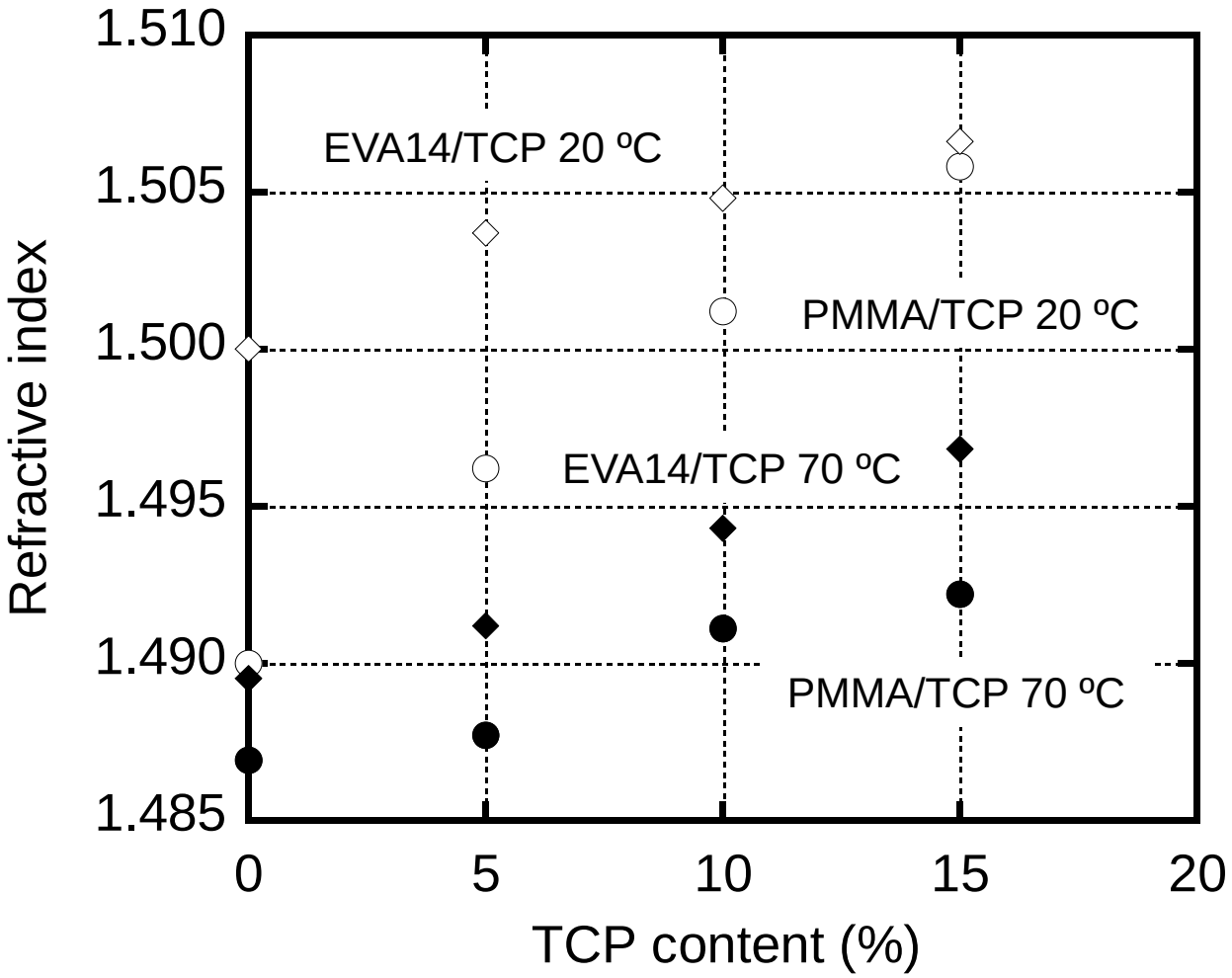

Takahashi et al.,

Figure 7

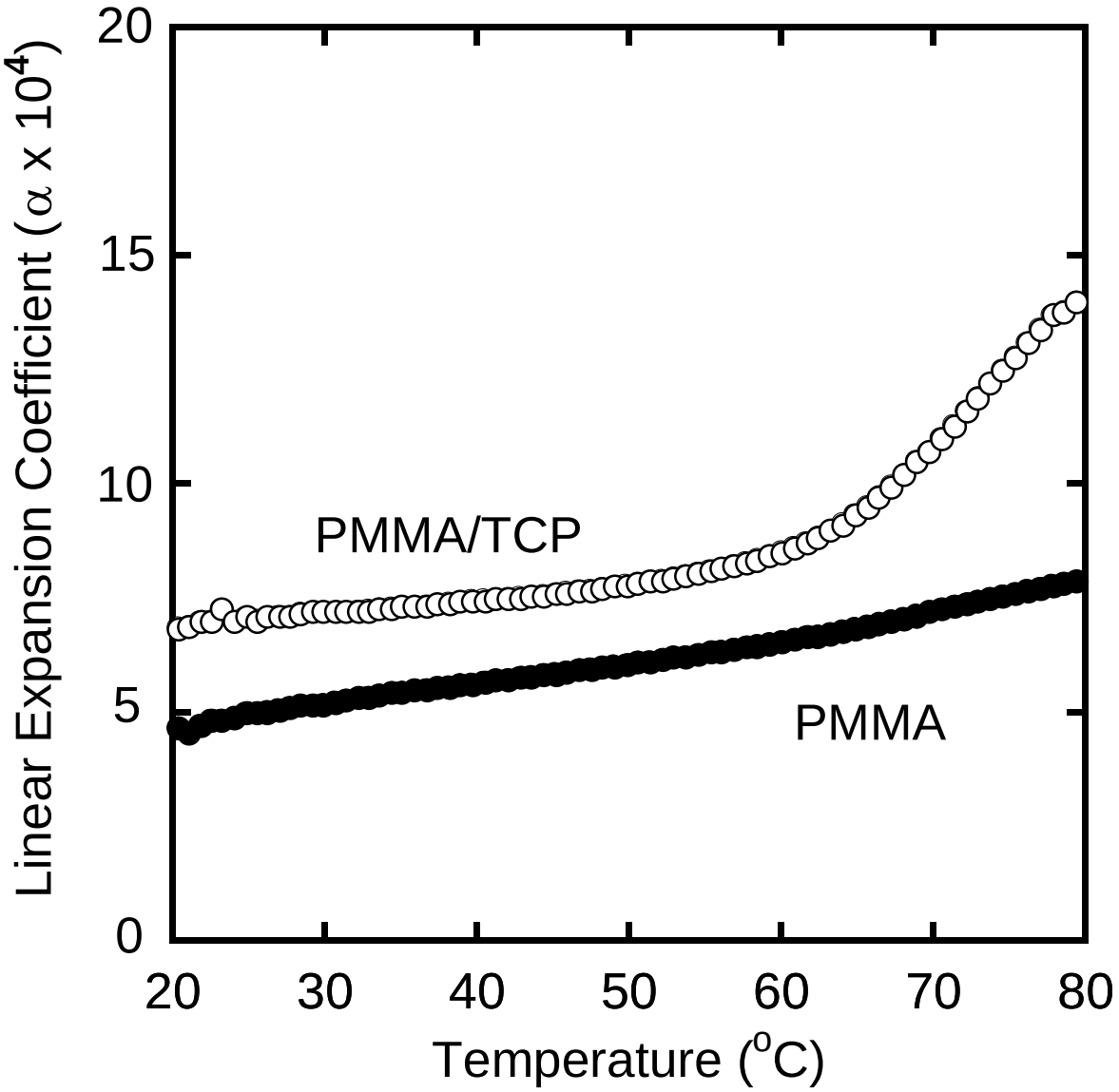

Takahashi et al.,

Figure 8

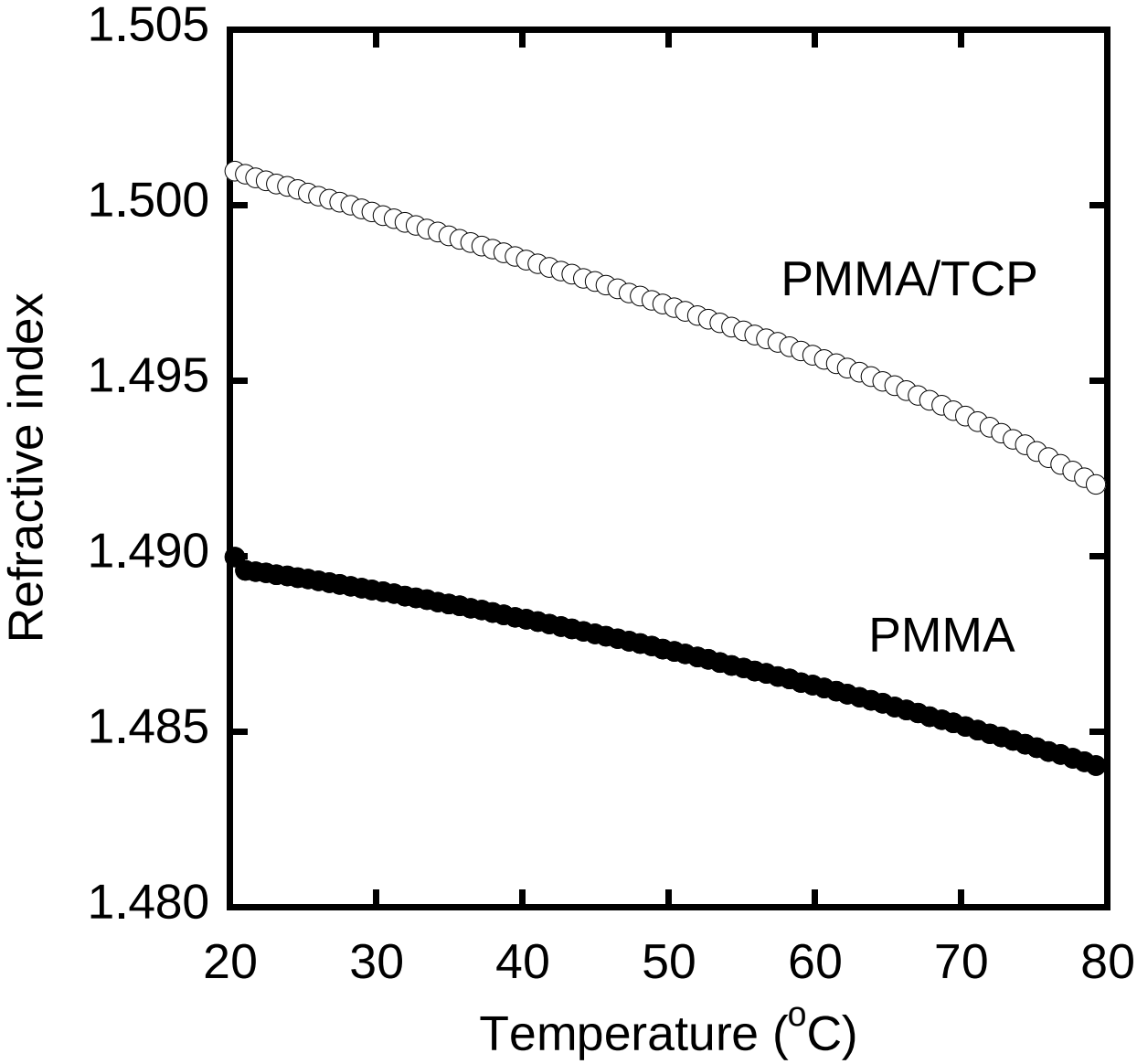

Takahashi et al.,

Figure 9

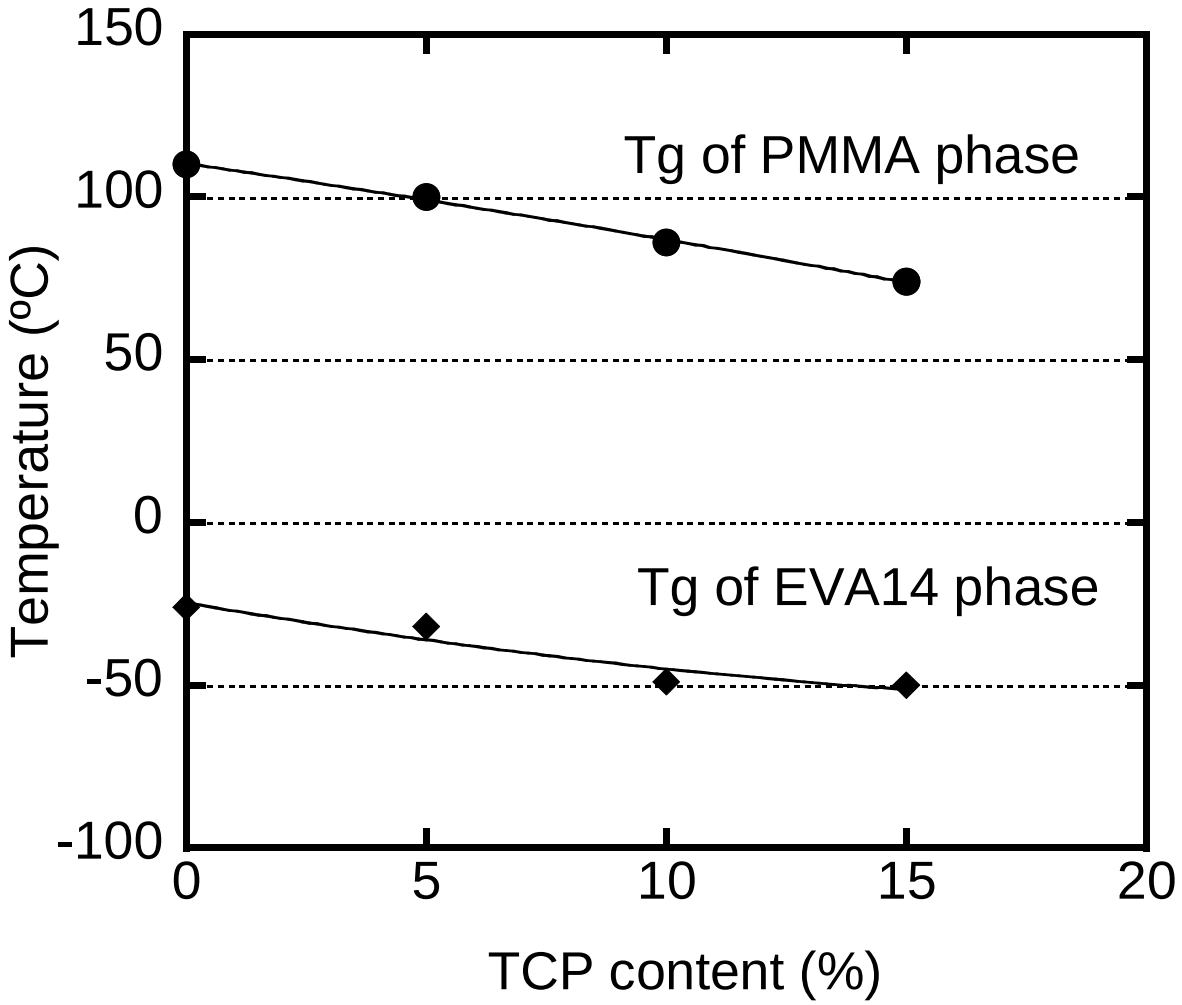

Takahashi et al.,

Figure 10

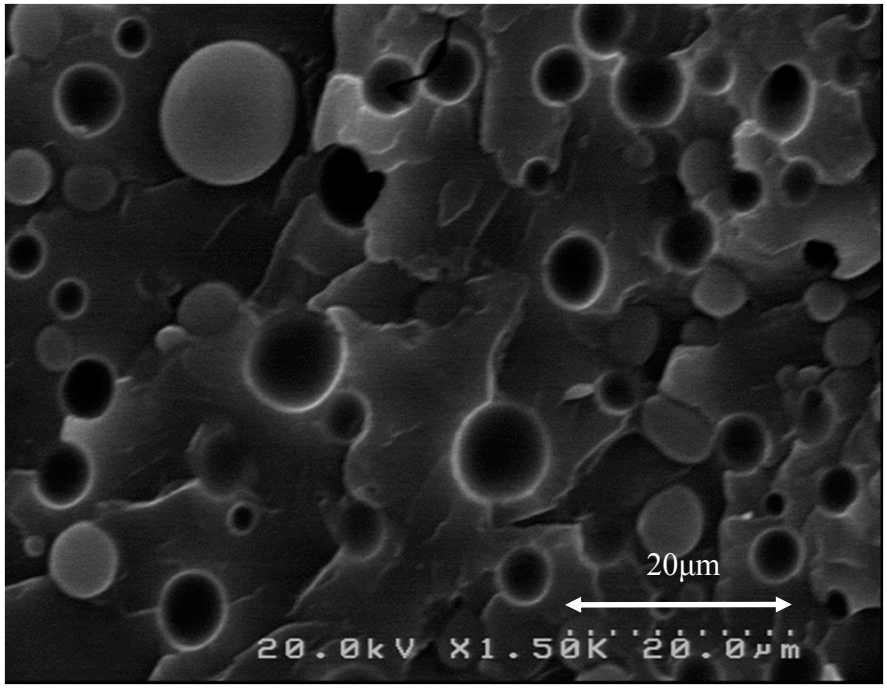

Takahashi et al.,

Figure 11

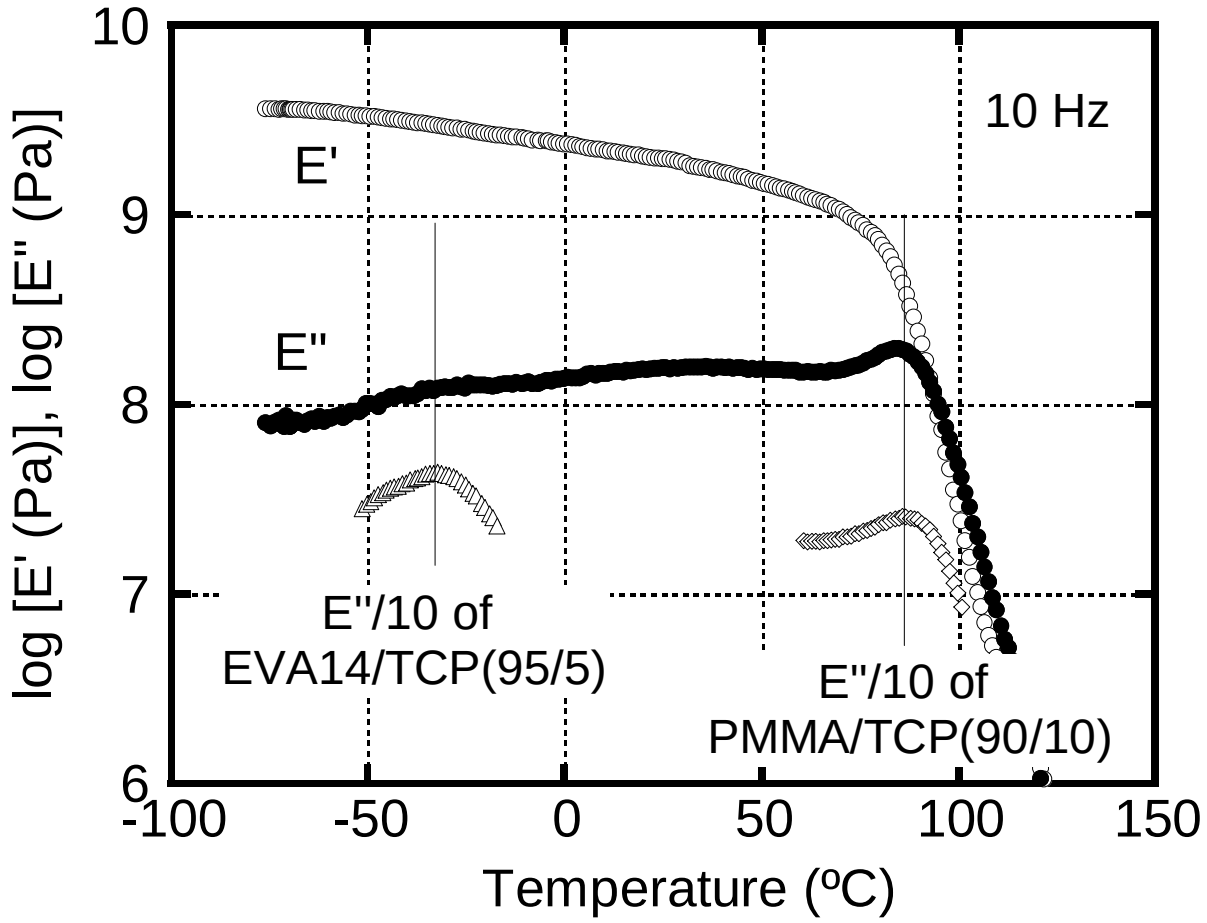

Takahashi et al.,

Figure 12